

Technical University of Denmark



Simulation-aided investigation of beam hardening induced errors in CT dimensional metrology

Tan, Ye; Kiekens, Kim; Welkenhuyzen, Frank; Angel, Jais Andreas Breusch; De Chiffre, Leonardo; Kruth, Jean-Pierre; Dewulf, Wim

Published in:

The 11th International Symposium of Measurement Technology and Intelligent Instruments

Publication date:

2013

[Link back to DTU Orbit](#)

Citation (APA):

Tan, Y., Kiekens, K., Welkenhuyzen, F., Angel, J. A. B., De Chiffre, L., Kruth, J-P., & Dewulf, W. (2013). Simulation-aided investigation of beam hardening induced errors in CT dimensional metrology. In The 11th International Symposium of Measurement Technology and Intelligent Instruments

DTU Library

Technical Information Center of Denmark

General rights

Copyright and moral rights for the publications made accessible in the public portal are retained by the authors and/or other copyright owners and it is a condition of accessing publications that users recognise and abide by the legal requirements associated with these rights.

- Users may download and print one copy of any publication from the public portal for the purpose of private study or research.
- You may not further distribute the material or use it for any profit-making activity or commercial gain
- You may freely distribute the URL identifying the publication in the public portal

If you believe that this document breaches copyright please contact us providing details, and we will remove access to the work immediately and investigate your claim.

Simulation-aided investigation of beam hardening induced errors in CT dimensional metrology

Ye Tan^{1,2}, Kim Kiekens^{1,2}, Frank Welkenhuyzen², J. Angel³, L. De Chiffre³, Jean-Pierre Kruth²
and Wim Dewulf^{1,2,*}

¹ Group T, KU Leuven Association, A.Vesaliusstraat 13, 3000 Leuven, Belgium

² Katholic University Leuven, Celestijnenlaan 300B, 3001 Heverlee, Belgium

³ Department of Mechanical Engineering, Technical University of Denmark, Building 425, Produktionstorvet, 2800 Kgs. Lyngby, Denmark

* Wim Dewulf / E-mail: Wim.Dewulf@mech.kuleuven.be

KEYWORDS : X-ray Computed Tomography, simulation, beam hardening

Industrial X-ray CT systems are increasingly used as dimensional measuring machines. However, micron level accuracy is not always achievable yet. The measurement accuracy is influenced by many factors, such as workpiece properties, X-ray settings, beam hardening and calibration methods [1-4]. Since most of these factors are mutually correlated, it remains challenging to interpret measurement results and to identify the distinct error sources. Since simulations allow isolating the different affecting factors, they form a useful complement to experimental investigations.

Dewulf et.al [5] investigated the influence of beam hardening correction parameters on the diameter of a calibrated steel pin in different experimental set-ups. It was clearly shown that inappropriate beam hardening correction can result in significant dimensional errors. This paper confirms these results using simulations of a pin surrounded by a stepped cylinder: a clear discontinuity in the measured diameter of the inner pin is observed where it enters the surrounding material. The results are expanded with an investigation of the beam hardening effect on the measurement results for both inner and outer diameters of the surrounding stepped cylinder. Accuracy as well as the effect on the uncertainty determination are discussed. The results are compared with simulations using monochromatic beams in order to have a benchmark which excludes beam-hardening effects.

In the final part of the paper, the investigations are expanded with experiments and simulations of new set-ups that include non-cylindrical features.

NOMENCLATURE

BH = beam hardening

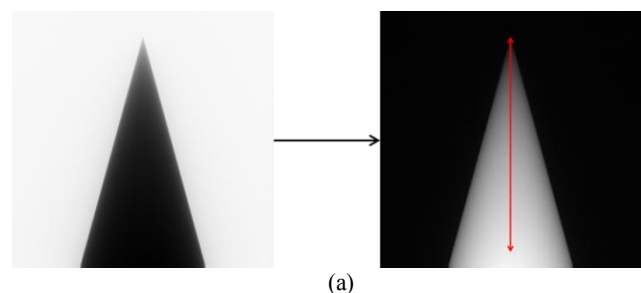
BHC = beam hardening correction

average frequency of the X-rays is shifted in the direction of higher energy during the propagation process; this is referred to as “hardening” of the X-ray beam. Because of the beam hardening (BH) effect, the X-ray attenuation is not strictly linearly related to the penetrated material thickness [5] (Fig. 1).

1. Introduction

1.1 Beam hardening effect

Most industrial X-ray tubes generate a polychromatic X-ray beam which is characterized by a continuous energy spectrum with certain bandwidth. Due to the energy dependent attenuation, lower energy (soft) X-rays are more easily and rapidly absorbed than high energy (hard) X-rays as the beam passes through a workpiece. Thus, the



(a)

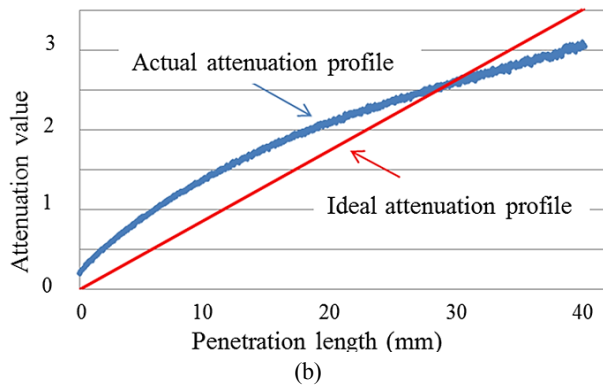


Fig. 1 (a) 2D X-ray projection image of a steel cone: pixel intensity values (gray values) are converted to X-ray attenuation values (the ability of attenuating X-ray beams); (b) Attenuation profile along the “red line” in (a).

1.2 Beam hardening correction

Most reconstruction algorithms presume linear relationship between X-ray attenuation and X-ray penetration length; as a result, non-linear artifacts such as cupping effect (Fig. 2) and dark streaks (Fig. 3) are generated after reconstruction due to the BH effect. These artifacts strongly degrade image quality, and hinder accurate material analysis and defect detection.

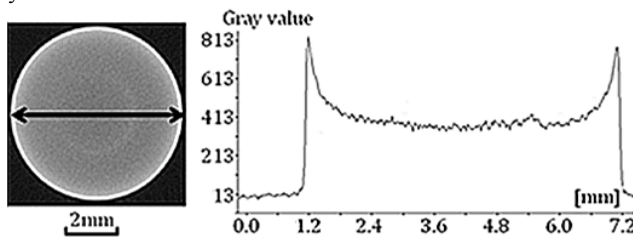


Fig. 2 Reconstructed slice of a steel cylinder and corresponding grey value profile along the arrow line [5].

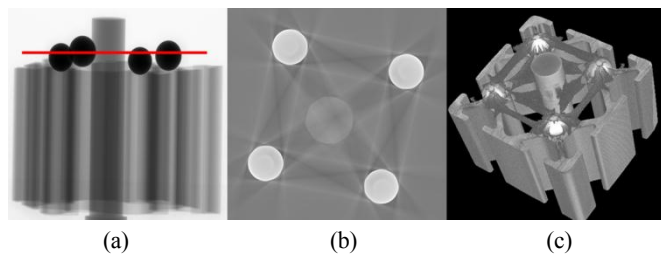


Fig. 3 (a) 2D X-ray image of an aluminum profile with four steel spheres; (b) streak artifacts visible in a reconstructed CT slice of the red section in (a); (c) 3D CT voxel model of the objects [5].

Many approaches have been developed for beam hardening correction (BHC); ranging from the most basic hardware filtration method to advanced iterative reconstruction algorithms [6, 7]. However, taking the computational cost and effectiveness into consideration, the linearization technique using pre-defined polynomials combined with hardware pre-filtration is favored by most industrial users. Currently, polynomials up to the fourth order are being used:

$$Y = a (b + cX + dX^2 + eX^3 + fX^4) \quad (1)$$

Where X represents the initial grey value of a pixel in an X-ray projection image, Y represents the final grey value after linearization, and “a” through “f” represent coefficients that can be fine-tuned depending on the severity of BH effect. A number of experience based BHC presets (up to second order) are listed in Table 1 [5].

Presets	Parameters					
	a	b	c	d	e	f
1	1	0	1	0	0	0
2	1	0	0.75	0.25	0	0
3	1	0	0.5	0.5	0	0

Table 1. Experience based BHC presets. Nr.1 keeps the original data; Nr.2 applies moderate BHC; Nr. 3 applies the severest BHC.

2. BHC for dimensional metrology

2.1 Necessary or Not

BHC can largely improve the image quality and makes the grey value of the same material appear uniform after reconstruction. On the other hand, the BH effect enhances edge contrast [8], since the material outer surface experiences a rapid gray value change; which is beneficial for material outer surface determination. The question remains: whether BHC is beneficial for dimensional metrology applications.

2.2 Experimental investigation: the influence of BHC on “internal” dimensions

The main power of industrial CT for dimensional metrology relies on its ability to measure internal features non-destructively. Thus, a simple setup (Fig. 4) has been used to investigate the influences of BHC on the measurement accuracy and uncertainty of internal dimensions. The main machine settings for scanning this setup are listed in Table 2.

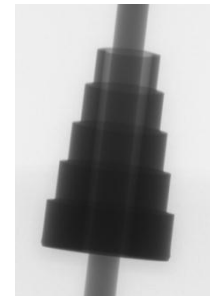


Fig. 4 2D X-ray projection image of the test setup: a calibrated stainless steel pin (Ø4 mm, dimensional tolerance $\pm 1 \mu\text{m}$) is partly surrounded by a stainless steel step cylinder. Thus, the middle part of the inner pin can be considered as an “internal” feature.

Voltage (KV)	Current (μA)	Copper filter (mm)
200	180	2

Table 2. Main machine settings for the setup in Fig. 4.

The original scan data (2D X-ray projections) are initially reconstructed using BHC preset Nr.1 (no correction) and Nr.2 (moderate correction). After local adaptive surface determination, proper object alignment and voxel size correction, the diameter of the middle pin is measured at equidistant slices from top to bottom. Fig. 5 plots the dimensional error (difference between the CT measured value and the reference value of Ø4mm) against the slice number (position where the measurements are taken: from top to bottom).

Similar to our previous report [5], local dimensional variations are observed when the pin “enters and leaves” the surrounding step cylinder. Such “jump” is around $4 \mu\text{m}$ if no BHC is applied, and around $10 \mu\text{m}$ if applying BHC preset Nr.2 (as listed in Table 1). The

major cause is that the surrounding material acts as an extra filter. As a result, the level of BH effect along the middle pin differs depending on the location. The difference of BH level results in a difference of edge offsets; this appears as a “jump” seen in Fig. 5. Non-proper BHC and especially over-correction can enlarge the difference between the inner and outer edge offsets and worsen the measurement uncertainty.

It can be noticed that the direction of the “jump” is inverted for BHC preset Nr.1 and Nr.2. It indicates that BHC preset Nr.1 has insufficient correction, whereas and BHC preset Nr.2 has over-correction; this makes it possible to eliminate these “jumps” by fine tuning the coefficients of the BHC polynomial. After 2 iterations, the “optimal” BHC coefficients are obtained: $a=1$, $b=e=f=0$, $c=0.85$ and $d=0.15$ (see Table 1). Significant improvement on the dimensional measurement results is achieved. As shown in Fig. 5, if we apply a constant edge offset correction term on the “purple line”, the overall dimensional errors are within $2.5\mu\text{m}$. This is very close to the dimensional tolerance of the pin: $\pm 1\mu\text{m}$.

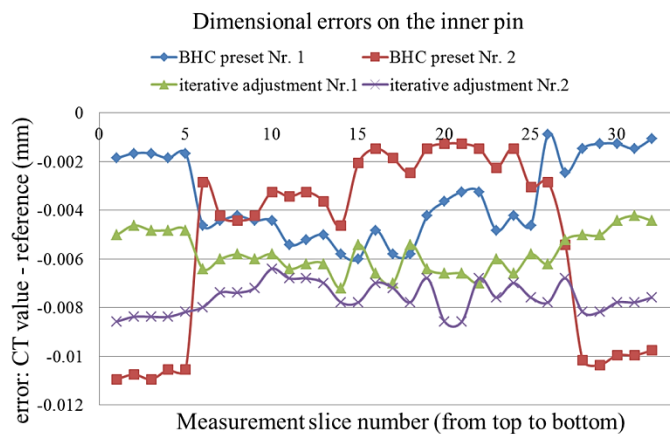


Fig. 5 Comparison of dimensional measurement errors on the inner pin (shown in Fig. 4) using different BHC coefficient sets. Attention: BHC preset Nr.1 – no correction.

2.3 Simulation verification

In order to clearly identify and investigate the influence of the BH effect and of BHC on the dimensional measurement results, it is necessary to eliminate other influencing factors, such as: X-ray scattering, machine axes alignment and focal spot drifting. These conditions are almost impossible to achieve experimentally, but can be easily realized by X-ray CT simulation. By using the BAM-aRTist simulation software, a CT scan of the same object (Fig. 4) is simulated under the same machine settings (X-ray voltage, current, filter and magnification), without X-ray scattering and focal spot drift. During reconstruction, the BHC coefficient sets used in Section 2.2 are reused to process the simulated data. Moreover, an X-ray source with a monochromatic spectrum is also simulated to serve as a benchmark, since it excludes BH effects.

After local adaptive thresholding and setting up work coordinates, the inner pin diameter is measured in the same way as in Section 2.2. The measurement results are shown in Fig. 6.

In general, the simulated measurement results coincide with the real measurements. Local dimensional variations are observed when the pin “enters” and “leaves” the surrounding step cylinder if BHC preset Nr.1 and Nr.2 are applied. By fine tuning the coefficients of the BHC polynomial, the dimensional measurement results can be

improved significantly to a level that is comparable with the results of an ideal X-ray source (monochromatic beam).

In general, the simulated measurement results coincide with the real measurements. Local dimensional variations are observed when the pin “enters” and “leaves” the surrounding step cylinder if BHC preset Nr.1 and Nr.2 are applied. By fine tuning the coefficients of the BHC polynomial, the dimensional measurement results can be significantly improved, which is comparable with the results of an ideal X-ray source (monochromatic beam).

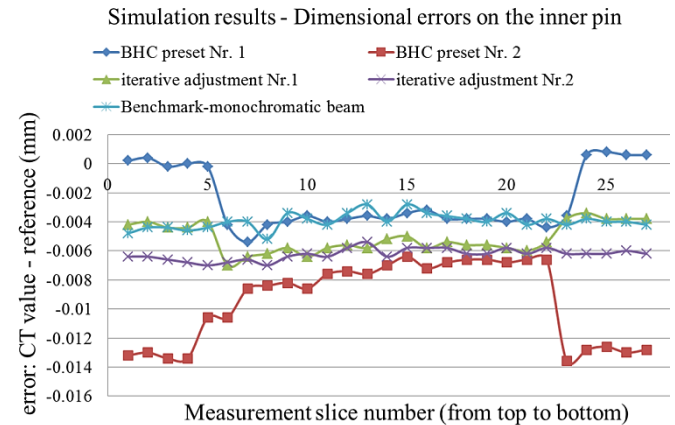


Fig. 6 X-ray CT simulation measurement results - Comparison of dimensional measurement errors on the inner pin (shown in Fig. 4) using different BHC coefficient sets.

2.4 Analysis and summary of the previous results

From the above results, we can conclude that appropriate BHC is useful for dimensional metrology applications. As shown in Fig. 5, the non-systematic errors are reduced from $6\mu\text{m}$ to $2\mu\text{m}$ by applying proper BHC. However, one has to be very careful not to over-correct the BH effect. Otherwise, the local dimensional variations might increase, for example with BHC preset Nr.2 (Fig. 5 and Fig. 6).

BH effect is closely related to the “cupping effect”. Two reconstructed slices (as shown in Fig. 7-a, Section 1 represent the outer part, Section 2 represent the inner part), are selected for investigating the influence of different BHC coefficients sets on the “cupping effect”. The gray value profiles (after reconstruction) along the “red line” are plotted in Fig. 7-b for 3 different BHC coefficients sets. If we don’t apply BHC (preset Nr.1), there is an obvious difference between inner and outer attenuation profile. The difference is reflected by the $4\mu\text{m}$ “jump” in Fig. 5. Applying BHC preset Nr.2 seemingly eliminates the cupping effect; however, the original gray values are significantly magnified. Moreover, over-correction can be observed (a small raise at the middle part of the blue line – Section 1). By fine tuning the coefficients of the BHC polynomial, it is possible to eliminate the cupping effect without magnifying the noise.

If comparing Fig. 5 (real measurement) and Fig. 6 (simulation), it can also be noticed that in the real measurements, the non-systematic noise is much worse than in the simulated data. The major cause is related to the exclusion of X-ray scattering in our simulations. Furthermore, even under the ideal situation with monochromatic X-ray beams, there is an edge offset of $4\mu\text{m}$ (Fig. 6). Although such systematic errors can easily be compensated, it proves that edge correction is necessary even without any artifacts and using local adaptive thresholding.

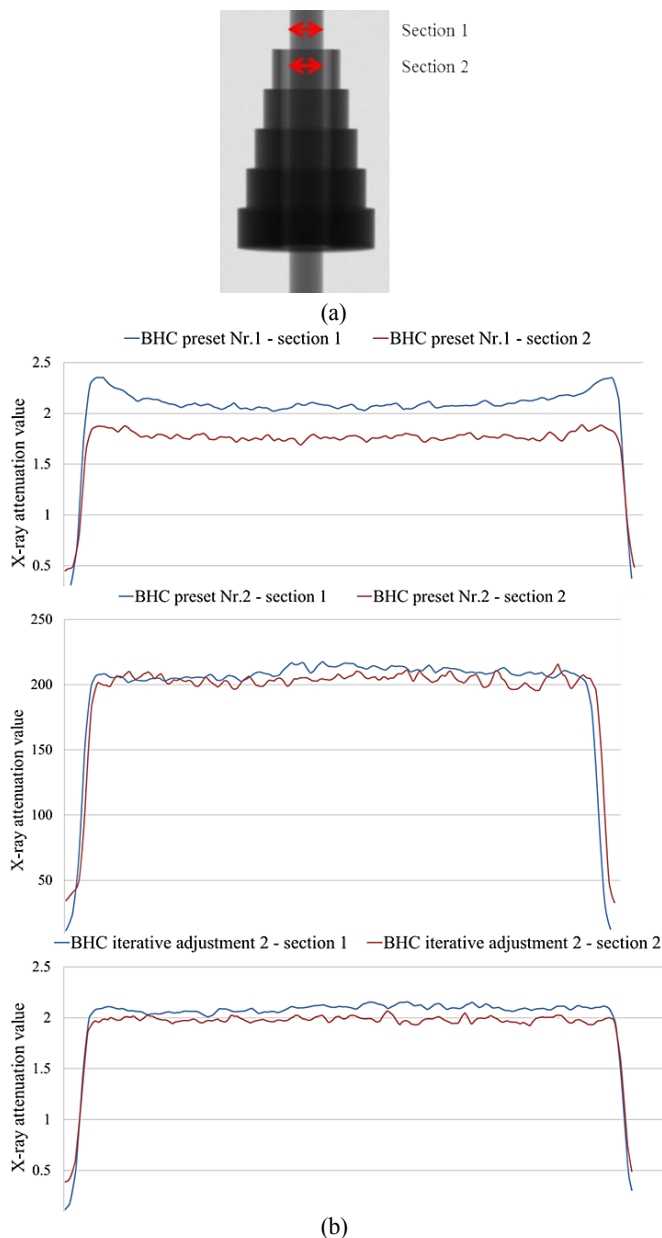


Fig. 7 (a) 2D X-ray projection image of the test object; (b) gray value profile taken on reconstructed slices (along the “arrow lines in (a)”) when applying BHC preset Nr.1, Nr.2 and the iterative adjustment Nr.2.

3. Calibration workpiece

3.1 Basic design concept

There are methods to determine the “best” BHC polynomial coefficients, for example by looking at the horizontal center slice on the X-ray detector, where the sum of total attenuation along the central slice should be equal for each scan angle. However, this method requires perfect alignment between X-ray source and detector, plus the maximum penetration length be placed at the center line (to ensure the optimization calculation covers the entire data range: from air to maximum attenuation), these constraints are not very practical; moreover, such method also has difficulties when dealing with purely cylindrical objects, because it makes use of the difference of each projection images which is much less with cylindrical objects.

As Section 2 concluded, it is possible to optimize the coefficients

of the BHC polynomial by minimizing the non-systematic dimensional errors on the middle pin. Meanwhile, we should also look at the influence of such BHC on the other dimensions, for example, the dimensional measurement errors on the step cylinder, to make sure that we do not improve the measurement results of one particular feature while worsening the others. If significant improvement on overall (including both the inner pin and the hollow step cylinder) dimensional measurement results can be obtained, then a simple workpiece as shown in Fig. 4 can be used for BHC calibration; because the “optimal” coefficients might be reused if an object of the same material and similar size is scanned under the same machine settings (X-ray voltage, current, filter...). Furthermore, the final dimensional errors detected on the outer features (step cylinder outer diameters) and inner features (step cylinder inner hole) could be used for edge offset calibration. In order to verify these assumptions, a more accurate stainless steel hollow step cylinder was manufactured and calibrated by tactile CMM. Its designed dimensions are shown in Fig. 8.

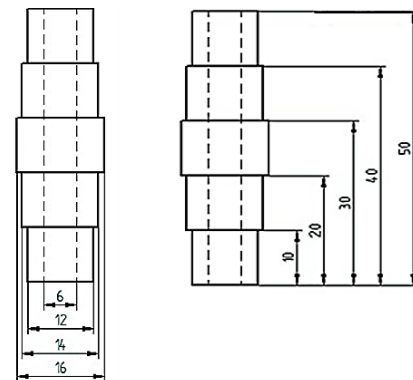


Fig. 8 The designed dimensions of the stainless steel hollow step cylinder. The complete calibration workpiece (shown in Fig. 9(a)) includes this step cylinder and the previously used stainless steel pin.

3.2 Dimensional measurement results

The complete calibration workpiece is shown in Fig. 9(a), it consists of the above mentioned hollow step cylinder (Fig. 8) and a well calibrated center pin (dimensional tolerance $\pm 1\mu\text{m}$). The machine settings for scanning this workpiece are listed in Table 3. X-ray CT simulation with the same settings but using monochromatic beam was performed and serves as a benchmark for comparison.

Voltage (KV)	Current (μA)	Copper filter (mm)
210	195	2

Table 3. Main machine settings for the setup in Fig. 9(a).

The diameter of the center pin is measured in the same way as described in Section 2.2 (circle diameters at equidistant slices from top to bottom); measurement results are shown in Fig. 9(b). The sudden “jumps” are used as a tool for defining the optimal coefficients for the BHC polynomial (iteratively adjusting the coefficients to eliminate these jumps). The inner hole and outer step cylinder diameters are also measured (as cylinders instead of circles) and plotted in Fig. 9(c). The idea is to check if the optimized BHC coefficients can also improve these dimensional measurement results; furthermore, they can be used for calculating the edge correction terms for internal and external features. From Fig. 9(b), we can see that the non-systematic dimensional errors are significantly reduced (from $7\mu\text{m}$ to $2\mu\text{m}$) after optimizing the BHC coefficients. The

difference between the “green line” and the “red line” (the monochromatic simulation results) might be due to the fact that the simulations are not “perfect” simulations of the actual object (material), detector, focal spot... Another reason is that X-ray scattering are excluded in our simulations. Similar results can be found on the step cylinder in Fig. 9(c): between BHC preset Nr.1 and optimized BHC coefficients, the average outer cylinder edge offsets are improved by around $3\mu\text{m}$ (from $5\mu\text{m}$ to $-2\mu\text{m}$); the edge offset of the inner hole is reduced by $8\mu\text{m}$ (from $-13\mu\text{m}$ to $-5\mu\text{m}$). Thus, after proper BHC, the overall dimensional (both systematic and non-systematic) errors are reduced to within $5\mu\text{m}$. This can be further improved by applying edge offset correction terms. The results prove that the simple setup (a well calibrated pin partly surrounded by another hollow cylinder) can function as BHC calibration object to optimize the coefficients of the BHC polynomial. The monochromatic CT simulation for this case was performed using simulation software developed at KULeuven.

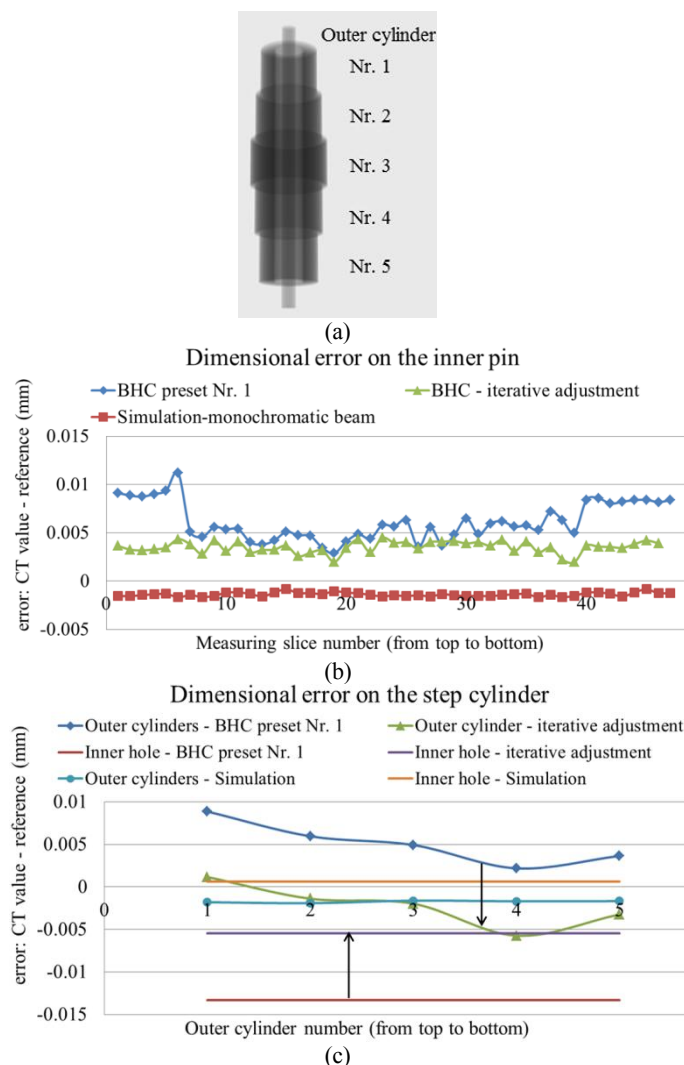


Fig. 9 (a) 2D projection image of the calibration workpiece; (b) dimensional errors on the inner pin: its diameter is measured (as circles) from top to bottom at equidistance slices; (c) dimensional errors on the step cylinder: the diameters of the 5 outer cylinders and the inner hole are measured (as cylinders) and compared with the CMM measurement results. For the results in both (b) and (c), the scan data of the real measurement are processed in two ways: without BHC (BHC preset Nr. 1), and with fine-tuned BHC coefficients: $a=1$, $b=e=f=0$, $c=0.82$ and $d=0.18$.

4. Case study

The calibration workpiece described in Section 3 can have two major functions:

1. If the target objects have the same material compositions, similar sizes and are scanned under the same machine settings (X-ray voltage, current, filter...), then the calibration workpiece can be used to optimize the coefficients of the BHC polynomial. This can help to minimize errors caused by BH effect.
2. The CT measurement errors on the inner hole and outer cylinders might be used to calculate the edge offset correction terms for bidirectional dimensions (dimensions that are sensitive to the surface determination).

4.1 Workpiece description

A stainless steel step gauge (Fig. 10) is used to test the above mentioned two functions of the calibration workpiece (shown in Fig. 9(a)). The designed dimensions are shown below:

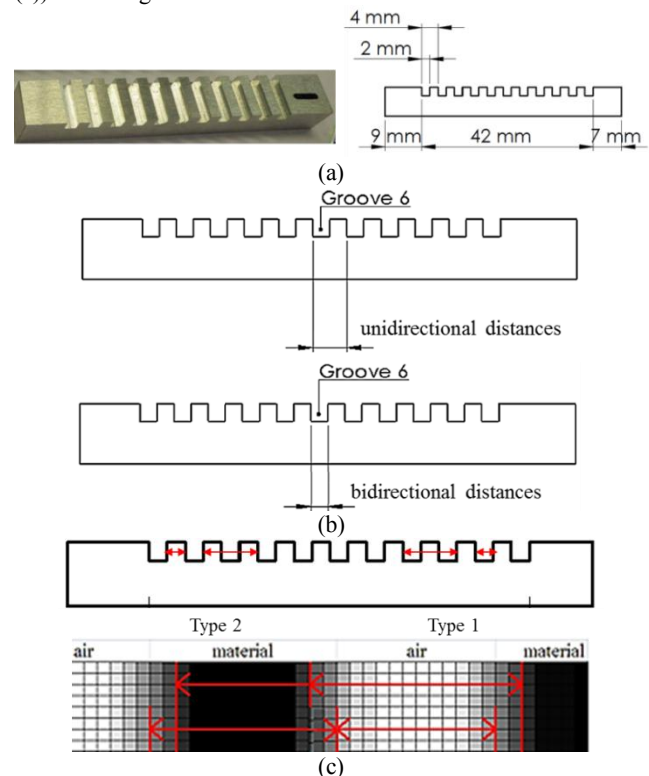


Fig. 10 (a) a photo of the step gauge and its designed dimensions; (b) indication of the unidirectional distances (edge independent) and bidirectional distances (edge dependent); (c) two types of edge dependent distances on the step gauge. Theoretically, type 1 and 2 have opposite edge offsets.

4.2 Dimensional measurement results

The step gauge is scanned using the same machine settings as the calibration workpiece. During reconstruction, the scan data are processed in two ways: without BHC (BHC preset Nr.1); and with “optimized” BHC polynomial coefficients (calculated from the calibration workpiece shown in Fig. 9(a)). After local adaptive surface determination and voxel size correction, 10 unidirectional distances and 11 bidirectional distances are measured and compared with reference CMM measurements. Moreover, an X-ray CT simulation with monochromatic beam has been performed and its results are set as the benchmark for analyzing the other measurement results.

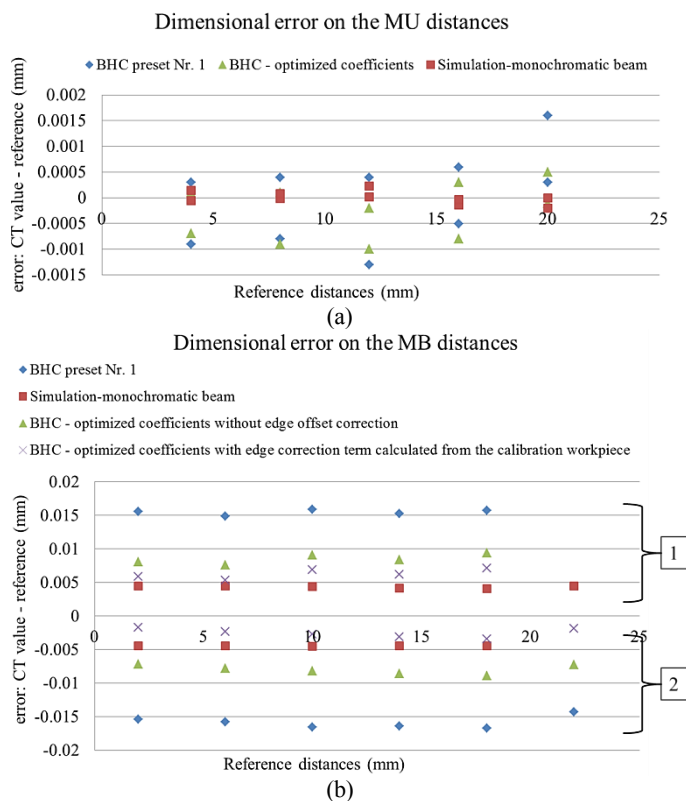


Fig. 11 (a) dimensional measurement results for 10 unidirectional distances: without BHC, with optimized BHC polynomial coefficients, and with monochromatic X-ray beam; (b) dimensional measurement results for 11 bidirectional distances: without BHC, with optimized BHC polynomial coefficients, monochromatic X-ray beam. The top half are “type 1” distances, the bottom half are “type 2” distances. Type 1 and 2 are as defined in Fig. 10(c).

There are several conclusions that can be drawn from Fig. 11(a):

1. The non-systematic errors are slightly reduced (from $3\mu\text{m}$ range to $1.5\mu\text{m}$ range) when applying the “optimized” BHC polynomial coefficients ($a=1$, $b=e=f=0$, $c=0.82$ and $d=0.18$, same as in Fig. 9 for the calibration workpiece).
2. Compared with the dimensional measurement results of the monochromatic X-ray beam simulation, there is still space for improvement; for example by reducing scattering noise, minimizing focal spot drifting and eliminating machine axes’ misalignment.

The information that we can get from Fig. 11(b) are:

1. When measuring distances between parallel planes, the positive and negative edge offset errors often have similar absolute value. Thus, the sum of two distances, one with positive edge offset and the other one with negative edge offset, are often used for voxel size correction. However, this trick cannot be generalized for objects with other kinds of features. Taking the calibration object (Fig. 9(a)) as an example (object with cylindrical features), the inner hole edge offset doesn’t necessarily equal the outer cylinder’s edge offset.
2. The optimized BHC polynomial coefficients calculated from the calibration workpiece can reduce the dimensional errors by half (variation range from $\pm 15\mu\text{m}$ to $\pm 7.5\mu\text{m}$).
3. Applying the edge offset terms (identified by the calibration workpiece) can improve the dimensional measurement results but cannot eliminate the edge errors completely. The cause could be that we are using edge correction terms calculated from cylinders to correct errors of plane distances.

5. Discussion and conclusion

This paper investigated the influence of BH effect and BHC on the dimensional measurement results for both internal and external features. The results verify our previous findings [5] which show that improper BHC can significantly worsen the accuracy and uncertainty of dimensional measurements.

Furthermore, a calibration workpiece (a hollow stepped cylinder together with a center pin, Fig. 9(a)) is developed for optimizing the coefficients of BHC polynomial and calculating the edge offset correction term. This concept is then tested using a stainless steel step gauge of similar size scanned under the same machine settings. On one hand, the optimized BHC coefficients turns out to be successful; on the other hand, the edge offset correction term calculated from the calibration workpiece can reduce but not completely eliminate the edge errors for plane distances. This might be due to feature dependent errors, differences in X-ray scattering and other influencing factors. The setup shown in Fig. 9(a) and the step gauge (Fig. 10) can both function as calibration workpiece for edge correction term calculation, while the former can also provide an experimental way to optimize the coefficients of BHC polynomial.

It is found through our investigation that internal and external features often have different edge offsets, this might be due to BH effect, X-ray scattering and the applied surface determination algorithm. Thus, single edge correction term is insufficient for objects with complex internal and external features.

It has to be mentioned that X-ray CT simulation plays an important role in helping us interpret our experimental results and identify the distinct error sources.

ACKNOWLEDGEMENT

The authors thank Dr. Carsten Bellon for his support with aRTist simulation software. Furthermore we acknowledge the support of the Research Foundation Flanders (FWO) via project G.0711.11 N and G.0618.10 and of the Flemish Agency for Innovation by Science and Technology (IWT) via project TETRA 120167.

REFERENCES

1. Kruth JP, Bartscher M, Carmignato S, Schmitt R, De Chiffre L, Weckenmann A “Computed Tomography for Dimensional Metrology,” Annals of the CIRP, Manufacturing Technology Vol.60(2):821–842, 2011.
2. Bartscher M, Hilpert U, Goebbels J, Weidemann G “Enhancement and Proof of Accuracy of Industrial Computed Tomography (CT) Measurement,” Annals of the CIRP, Manufacturing Technology 56(1):495–498, 2007.
3. De Chiffre, L., Hansen, H.N., Morace R.E., “Comparison of Coordinate Measuring Machines using an Optomechanical Hole Plate,” Annals of the CIRP, 54/1:479-482, 2005.
4. Schmitt, R., Niggemann, C., “Uncertainty in measurement for X-ray-computed tomography using calibrated work pieces,” Measurement Science and Technology, 21 (5), 2010.
5. Dewulf W, Tan Y, Kiekens K “Sense and non-sense of beam hardening correction in CT metrology,” Annals of the CIRP, Manufacturing Technology, Vol.61 (1): 495-498, 2012.

6. Krumm M, Kasperl S, Franz M “Referenceless Beam Hardening Correction in 3D Computed Tomography Images of Multi-Material Objects,” 17th World Conf. on Non-destructive Testing, Shanghai, China, 2008.
7. Amirkhanov A, Heinzl C, Reiter M, Kastner J, Groller E “Projection-Based Metal-Artifact Reduction for Industrial 3D X-ray Computed Tomography,” IEEE Trans. on Visualization and Computer Graphics, Vol 17, 2011.
8. Van de Castele, E. “Model-based Approach for Beam Hardening Correction and Resolution Measurements in Microtomography”, PhD Thesis, University of Antwerp, 2004.